Published in Materials & Design 2006

A class of slipline field solutions for extrusion through wedge shaped dies with slipping friction

N.S. Das, K.P. Maity *

Department of Mechanical Engineering, Regional Engineering College, National Institute of Technology, Rourkela 769008, Orissa, India

Abstract

In extrusion process, plastic deformation is achieved by applying force to a block of metal through a suitable die which results in reduction of the cross section of the product. A great deal of effort has been made at theoretical evaluation of deformation process using different techniques like Finite Element Modelling, weighted residual method and upper bound method, which yield approximate solution. The theory of slipline field has now advanced to a highly developed state and has been successfully utilized in the analysis of deformation modes of extrusion process. In the present analysis, the slipline field solutions have been obtained for slipping friction at the die metal interface for wedge shaped die. All solutions are analysed over the complete range of reductions. The mean extrusion and die pressures are computed for a number of die geometries and for different frictional condition at the interface.

Keywords: Extrusion; Slipline field; Wedge-shaped die

1. Introduction

Metal deformation through extrusion processes plays a key role in metal forming industries. It is highly essential to study the mode of metal deformation process exactly in the deformation process to satisfy the requirements of robust die design of extrusion processes. In the recent past, a great deal of techniques like FEM, weighted residual method and upper bound method [1–5] have been used in this connection. All the above methods can be applied to both 2D and 3D deformations, but the solutions obtained by the above methods are based on some approximations. In contrast to that the slipline field solutions yield exact solution, but only for plane strain deformation. It has attracted a number of researchers in the field of plastic deformation modeling to obtain exact solution.

Much attention has been devoted in the past to the study of the mechanics of metal extrusion through wedge shaped dies using slipline field solutions. In the slipline field solutions for drawing/extrusion through smooth wedge-shaped dies it is observed that the field with straight lines and circular arcs which applies for lower reductions, fails for certain higher reductions when the velocity discontinuity terminates on the exit slipline as shown by Hill and Tupper [6]. Solutions for these reductions involving curved exit sliplines were proposed by Green [7] from an analogy with the problem of plane strain compression between smooth parallel plates where, simple straight-line fields occur for integral values of width to thickness ratios and, for intermediate values, fields with curved exit sliplines apply. These indirect solutions for the case of drawing through frictionless dies were analysed by Dewhurst and Collins [8] and Venter, Hewitt and Johnson [9] who computed the mean drawing stress for a number of die geometries and also established the oscillatory behavior of the redundant work factor, similar to that observed in the case of plane strain compression between smooth parallel plates [7].

For short dies, the slipline fields can be constructed starting from straight lines and circular arcs and these fields for the case of smooth dies were analysed by Hill and

* Corresponding author. Tel.: 916612462510; fax: 916612472926/2471169.
E-mail address: kpmaity@nitrkl.ac.in (K.P. Maity).

Tupper [6], Venter, Hewitt and Johnson [9] and by Chenot, Felgeres, Lavarenne and Salencon [10] who obtained results for the more complicated problem of axisymmetric extrusion. The effect of friction on drawing/extrusion pressure for these geometries was studied by Hill and Green [11], Bishop [12] and Johnson [13,14]. Upper bound to the mean pressures for these cases has also been computed by Green [15], Westwood and Wallace [16].

In this paper the above solutions are extended to the case of extrusion with slipping friction at the die metal interface ($\tau = mk$). All solutions are analysed over the complete range of reductions to which they apply and, mean extrusion and die pressures are computed for a number of die geometries and for different frictional conditions at the interfaces.

2. Slipline fields

The four slipline field configurations associated with extrusion of metals through wedge-shaped dies with slipping friction at the interface ($\tau = mk$) and designated as types I–IV solution are illustrated in Figs. 1–4, respectively. For a given die angle 'α' and for a given value of the friction factor 'm' each of these fields extend over a definite range of reduction.

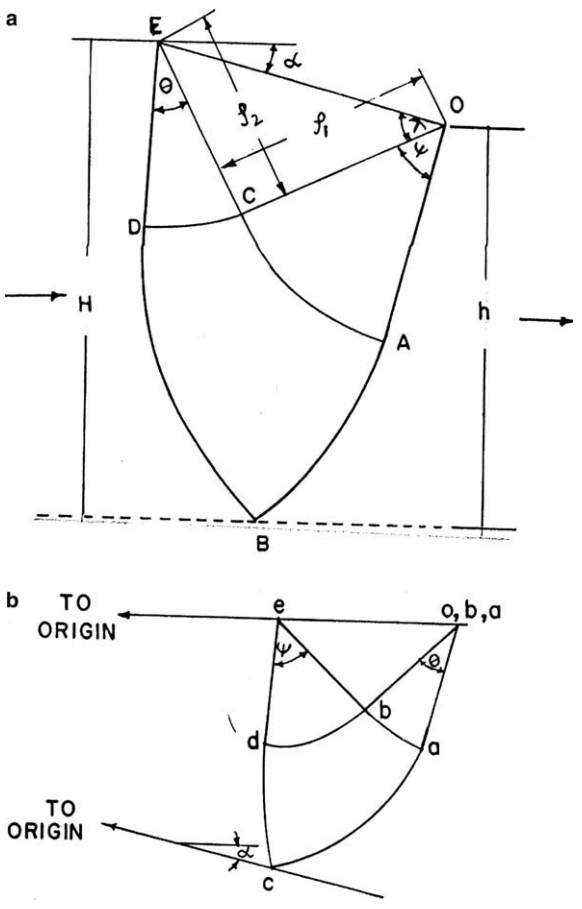

Fig. 1. (a) Slipline field type-I; (b) hodograph.

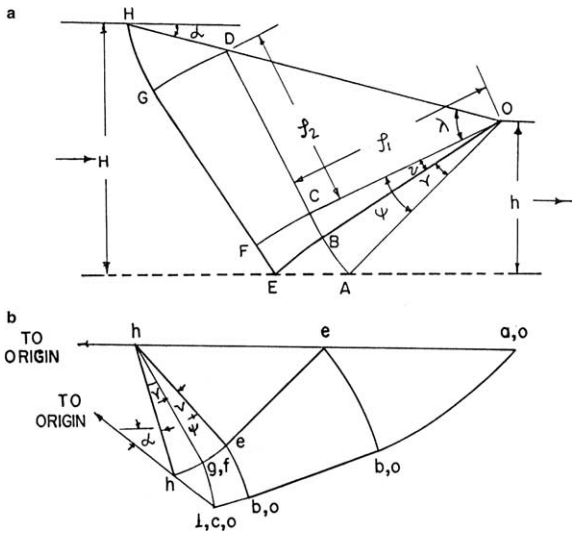

Fig. 2. (a) Slipline field type II; (b) hodograph.

Type I solution (Fig. 1(a)) applies when the fractional reduction 'r' is less than $2\sin\alpha/(\sqrt{(1+m)}+2\sin\alpha)$. The maximum reduction corresponds to the limiting field of Fig. 1 (a) for which $\theta = 0$. For reductions greater than the above value of slipline field of Fig. 1(a) can be continued in the manner demonstrated in Fig. 2(a) (type II solution). The limiting configuration of this solution is attained when the angular range of the sliplines equals $(\alpha + \eta)$ where, $m = \cos 2\lambda = \sin 2\eta$ (Fig. 2(c)).

Beyond the limiting configuration of Fig. 2(a), a different class of solutions apply as indicated by Green [7]. These solutions involving curved exit sliplines are the types III and type IV solution as shown in Figs. 3 and 4, respectively. The solution of Fig. 3 applies when the reduction is greater than that corresponding to the limiting field of Fig. 2(a) while, the solution of Fig. 4 applies when the reduction is less than a limiting value. The characteristic feature of these solutions is that they involve velocity discontinuities along certain slipline curves and also tramline regions where one family of sliplines are straight. Solutions for still greater reductions can be obtained by continuing construction beyond the limiting field. These solutions, however, are more of theoretical interest since, dies of such geometries are rarely used for extrusion or drawing of metals.

3. Series representation of slipline curves

In the present study, the above solutions are analysed with the help of the matrix method, for different frictional conditions on the die faces. For the direct solutions of Figs. 1 and 2 the radius of curvature of the different slipline curves could be readily calculated starting from the circular arc AC. For the indirect solutions of Figs. 3 and 4, the matrix inversion procedure was followed to determine the base slipline. In the following sections the governing equa-

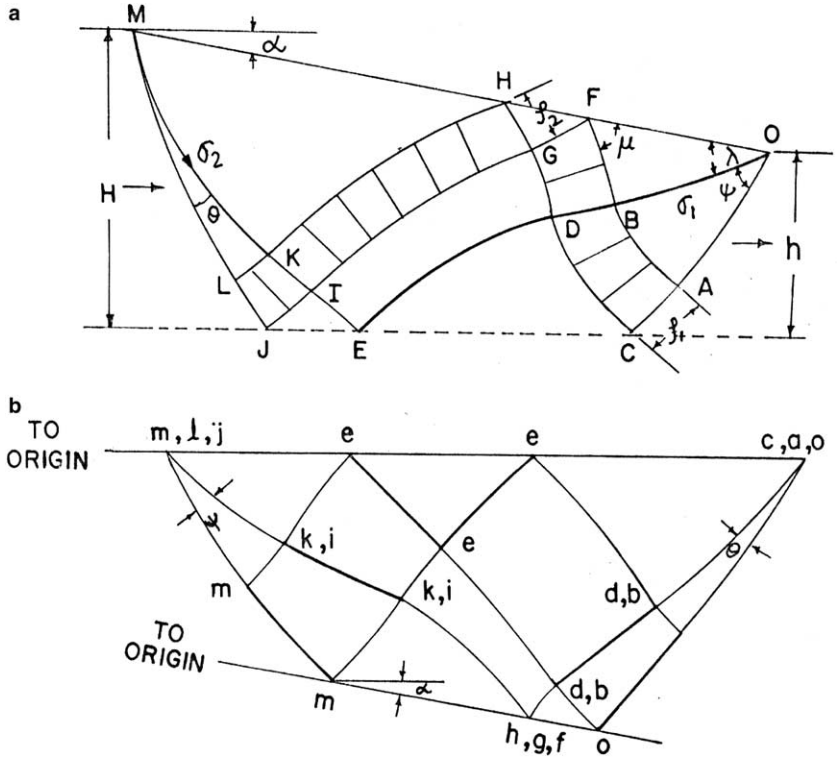

Fig. 3. (a) Slipline field type III; (b) hodograph.

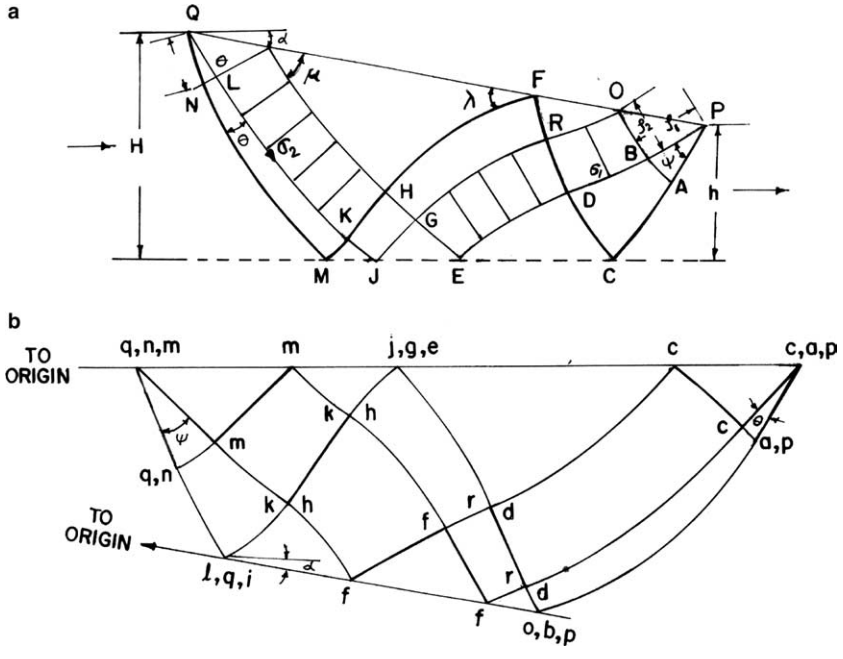

Fig. 4. (a) Slipline field type IV; (b) hodograph.

tions for these solutions are presented for evaluation of coordinates and load variables.

3.1. Slipline field type I

Referring to Fig. 1(a), CA and CD are circular arcs of radius ρ_1 and ρ_2, respectively. Hence, with the sign convention used for the slipline curvature these slipline curves can be represented by,

$$\begin{aligned} \mathrm{CA} &= \rho_1 c \\ \mathrm{CD} &= -\rho_2 c, \end{aligned} \tag{1}$$

where $\rho_2 = \rho_1 \tan\lambda$ and c represents a circle of unit radius. From the slipline net CABD, slipline curves BA and DB

can be calculated by constructing singular fields about CA and CD. Thus

$$\mathrm{BA} = (\rho_1 Q_{\psi\theta} - \rho_2 P_{\theta\Psi})c,$$

and

$$\mathrm{DB} = (\rho_1 P^*_\theta - \rho_2 Q^*_\theta)c. \tag{2}$$

The equations for the evaluation of force and geometrical parameters for this field are given as,

Thickness of the extruded sheet :

$$h = X_{\mathrm{BA}} \sin \pi/4 + Y_{\mathrm{BA}} \cos \pi/4 + \rho_1 \sin(\pi/4 + \theta)$$

Thickness of the billet :

$$H = X_{\mathrm{DB}} \cos(\pi/4 - \psi) - Y_{\mathrm{DB}} \sin(\pi/4 - \psi) + \rho_2 \cos(\pi/4 - \psi)$$

Extrusion force :

$$\begin{aligned} F/k = {} & FX_{\mathrm{DB}} \sin(\pi/4 - \psi) + FY_{\mathrm{DB}} \cos(\pi/4 - \psi) \\ & + \rho_2(P_{\mathrm{D}} \cos(\pi/4 - \psi) - \sin(\pi/4 - \psi)), \end{aligned} \tag{3}$$

where the field angle ψ is given by relation, $\psi = \pi/4 + \alpha + \theta - \lambda$ and, P_{D} is the hydrostatic pressure at D.

3.2. Slipline field type II

Referring to Fig. 2(a), AC is a circular arc of radius ρ_1. Hence,

$$\mathrm{AC} = -\rho_1 c.$$

The radius of curvature of other slipline curves are calculated with the help of the following equations:

$$\begin{aligned} \mathrm{FC} &= -\rho_1 S_\upsilon T^1_\psi c \\ \mathrm{FE} &= -\rho_1 R_\upsilon T_\upsilon T^{-1}_\psi c \\ \mathrm{GD} &= -(\rho_1 S_\upsilon T^{-1}_\psi + \rho_2)c \\ \mathrm{DG} &= -R_\gamma(\rho_1 S_\gamma T^{-1}_\psi + \rho_2)c \\ \mathrm{HG} &= -G_{\lambda\gamma} R_\gamma(\rho_1 S_\upsilon T^{-1}_\psi + \rho_2)c \end{aligned} \tag{4}$$

where

$$\psi = \gamma + \upsilon.$$

Thickness of the extruded sheet :

$$h = \cos \frac{\pi}{4}$$

Thickness of the billet :

$$\begin{aligned} H = {} & X_{\mathrm{HG}} \cos(\pi/4 - \psi) - Y_{\mathrm{HG}} \sin(\pi/4 - \psi) \\ & + \rho_2 \cos(\pi/4 - \upsilon) + X_{\mathrm{FE}} \cos(\pi/4 - \upsilon) \\ & - Y_{\mathrm{FE}} \sin(\pi/4 - \upsilon) \end{aligned} \tag{5}$$

Extrusion force :

$$\begin{aligned} F/k = {} & FX_{\mathrm{HG}} \sin(\pi/4 - \psi) + FY_{\mathrm{HG}} \cos(\pi/4 - \psi) \\ & + \rho_2(P_{\mathrm{F}} \cos(\pi/4 - \upsilon) - \sin(\pi/4 - \upsilon)) \\ & + FX_{\mathrm{FE}} \sin(\pi/4 - \upsilon) + FY_{\mathrm{FE}} \cos(\pi/4 - \upsilon), \end{aligned}$$

where P_{F} is the hydrostatic pressure at F.

3.3. Slipline field type III

The base slipline MK and the slipline curve OB are designated by σ_2 and σ_1 (Fig. 3).

$$\begin{aligned} \mathrm{AB} &= Q_{\theta\psi}\sigma_1 \\ \mathrm{CD} &= Q_{\theta\psi}\sigma_1 - \rho_1 c \\ \mathrm{ED} &= T^{-1}_\psi(Q_{\theta\psi}\sigma_1 - \rho_1 c) \\ \mathrm{LK} &= Q_{\psi\theta}\sigma_2 \\ \mathrm{JI} &= Q_{\psi\theta} \\ \mathrm{EI} &= T^{-1}_\theta(Q_{\psi\theta}\sigma_2 + \rho_2 c) \\ \mathrm{FB} &= G^{-1}_{\mu\theta}\sigma_1 \\ \mathrm{HK} &= G^{-1}_{\lambda\psi}\sigma_2 \\ \mathrm{GD} &= G^{-1}_{\mu\theta}\sigma_1 + \rho_1 c \\ \mathrm{GI} &= G^{-1}_{\lambda\psi}\sigma_2 - \rho_2 c \\ \mathrm{EI} &= P_{\theta\psi}\mathrm{GD} - Q_{\psi\theta}\mathrm{GI} \\ \mathrm{ED} &= P_{\psi\theta}\mathrm{GI} - Q_{\theta\psi}\mathrm{GD} \end{aligned} \tag{6}$$

where $\psi = \pi/4 + \alpha - \lambda + \theta$, $\mu = \pi/2 - \lambda$ and G is the rough boundary operator.

The base slipline equation σ_2 is obtained from the following equation:

$$\begin{aligned} (CG_{\mu\theta}P^*_{-\psi}R_\theta A - D)\sigma_2 = {} & \rho_1(CG_{\mu\theta} - (Q_{\theta\psi} - T^{-1}_\psi))c \\ & + \rho_2(CG_{\mu\theta}P^*_{-\psi}R_\theta(Q_{\psi\theta} - T^{-1}_\psi) - P_{\psi\theta})c. \end{aligned} \tag{7}$$

The slipline curve σ_1 is obtained by substituting σ_2 in the following equation:

$$B\sigma_1 - A\sigma_2 + \rho_1 P_{\theta\psi} c + \rho_2(Q_{\psi\theta} - T^{-1}_\theta)c = 0, \tag{8}$$

where

$$\begin{aligned} A &= Q_{\psi\theta}G^{-1}_{\lambda\psi} + T^{-1}_\theta Q_{\psi\theta} \\ B &= P_{\theta\psi}G^{-1}_{\mu\theta} \\ C &= Q_{\theta\psi}G^{-1}_{\mu\theta} + T^{-1}_\psi Q_{\theta\psi}, \end{aligned}$$

and

$$D = P_{\psi\theta}G^{-1}_{\lambda\psi}.$$

The equations of for the force and the geometrical parameters for the slipline field are as follows:

$$\begin{aligned} h &= X_{\mathrm{OA}} \cos(\pi/4 - \theta) + Y_{\mathrm{OA}} \sin(\pi/4 - \theta) + \rho_1 \sin \pi/4 \\ H &= X_{\mathrm{ML}} \cos(\pi/4 - \psi) - Y_{\mathrm{ML}} \sin(\pi/4 - \psi) + \rho_2 \sin \pi/4 \\ F/k &= FY_{\mathrm{ML}} \cos(\pi/4 - \psi) + FX_{\mathrm{ML}} \sin(\pi/4 - \psi) \\ & \quad + \rho_2(P_{\mathrm{j}} \cos \pi/4 - \sin \pi/4), \end{aligned} \tag{9}$$

where P_{j} is the hydrostatic pressure at point j.

3.4. Slipline field type IV

Referring to Fig. 4(a), the base slipline LK is designated by σ_2 and the slipline curve BD by σ_1. BA and LN are circular arcs represented by

$$\begin{aligned} \mathrm{BA} &= \rho_1 c \\ \mathrm{LN} &= -\rho_3 c, \end{aligned}$$

where $\rho_3 = \rho_1 \tan^2 \lambda$.

Other slipline curves are calculated as follows:

$$\mathrm{CD} = \rho_1 P_{\psi\theta} c + Q_{\theta\psi} \sigma_1$$
$$\mathrm{ED} = T_{\psi}^{-1} (\rho_1 P_{\psi\theta} c + Q_{\theta\psi} \sigma_1)$$
$$\mathrm{GR} = T_{\psi}^{-1} (\rho_1 P_{\psi\theta} c + Q_{\theta\psi} \sigma_1) - \rho_2 c$$
$$\mathrm{MK} = Q_{\psi\theta} \sigma_2 - \rho_3 P_{\theta\psi} c$$
$$\mathrm{JK} = T_{\theta}^{-1} (Q_{\psi\theta} \sigma_2 - \rho_3 P_{\theta\psi} c)$$
$$\mathrm{GH} = T_{\theta}^{-1} (Q_{\psi\theta} \sigma_2 - \rho_3 P_{\theta\psi} c) + \rho_2 c.$$

The base slipline σ_2 is obtained from the following equation as follows:

$$\begin{aligned}(CG_{\mu\theta} P^*_{-\psi} R_\theta A - D)\sigma_2 = {} & \rho_2 (CG_{\mu\theta} P^*_{-\psi} R_\theta (B + Q_{\psi\theta} G^{-1}_{\lambda\psi} - I) \\ & - (D + Q_{\theta\psi} G^{-1}_{\mu\theta} - I))c \\ & + \rho_3 CG_{\mu\theta} P^*_{-\psi} R_\theta T_\theta^{-1} P_{\theta\psi} c - \rho_1 T_\psi^{-1} P_{\psi\theta} c.\end{aligned} \tag{10}$$

The slipline σ_1 is obtained by substituting σ_2 in the following equation

$$C\sigma_1 - D\sigma_2 + \rho_1 T_\psi^{-1} P_{\psi\theta} c + \rho_2 (D + Q_{\theta\psi} G^{-1}_{\mu\theta} - I)c = 0. \tag{11}$$

The equations for the calculation of the force and geometrical parameters for this field are as follows:

$$\begin{aligned} h &= (X_{\mathrm{AC}} + \rho_1) \cos(\pi/4 - \theta) + Y_{\mathrm{AC}} \sin(\pi/4 - \theta) \\ H &= (X_{\mathrm{NM}} + \rho_3) \cos(\pi/4 - \psi) - Y_{\mathrm{NM}} \sin(\pi/4 - \psi) \\ F/k &= FX_{\mathrm{NM}} \sin(\pi/4 - \psi) + FY_{\mathrm{NM}} \cos(\pi/4 - \psi) \\ &\quad + \rho_3 (P_N \cos(\pi/4 - \psi) - \sin(\pi/4 - \psi)) \end{aligned} \tag{12}$$

where P_{N} is the hydrostatic pressure at N.

4. Computation

For a given set of field angles, the base slipline σ_2 for type III solution was determined from Eq. (5) and for type IV solution from Eq. (8) by inversion of the matrix operator $(CG_{\mu\theta} P^*_{-\psi} R_\theta A - D)$. The radius of curvature of other slipline curves and the geometrical details of the fields were then calculated with the help of standard subroutines. In both cases, the hydrostatic pressure at point c (Figs. 3(a) and 4(a)) was obtained from the condition that the extruded product is stress free. The hydrostatic pressures at the origin of the bounding sliplines ML (type III solution) and NM (type IV solution) were then evaluated using Hencky's equation. The total traction on the bounding slipline was then calculated from which, the mean extrusion and die pressures were determined for the given geometry.

In this manner, results from the above indirect solutions were computed for various values of m between 0.1 and 0.9 and, for semi-wedge angle α of the dies between 5° and 60°. In view of small angular range of slipline curves, 6×6 truncated matrices were used for calculation. All programmes were run on an IBM 1130 computer and the time taken for calculation was approximately 5 min.

The geometry of each field is specified by the field angles θ, λ, semi-wedge angle α and the length ρ_1 of the exit slipline ($\psi = \pi/4 + \alpha + \theta - \lambda$). ρ_1 Being a scale factor was set equal to unity while, the value of λ was decided by the friction factor 'm' between the die metal interface ($m = \cos 2\lambda$). The range of possible values of ψ corresponds to the range of reductions for which the field is valid. For initial set of calculations, λ was taken equal to $\pi/4$ and the results were checked against those of Venter, Hewitt and Johnson [4] for the frictionless case.

For the direct solutions (types I and II), the radius of curvature of the various slipline curves were calculated from the circular arc CA using standard matrix operators and superposition principle. The force and the geometrical details were then evaluated with the help of the equations presented in Eqs. (3) and (5).

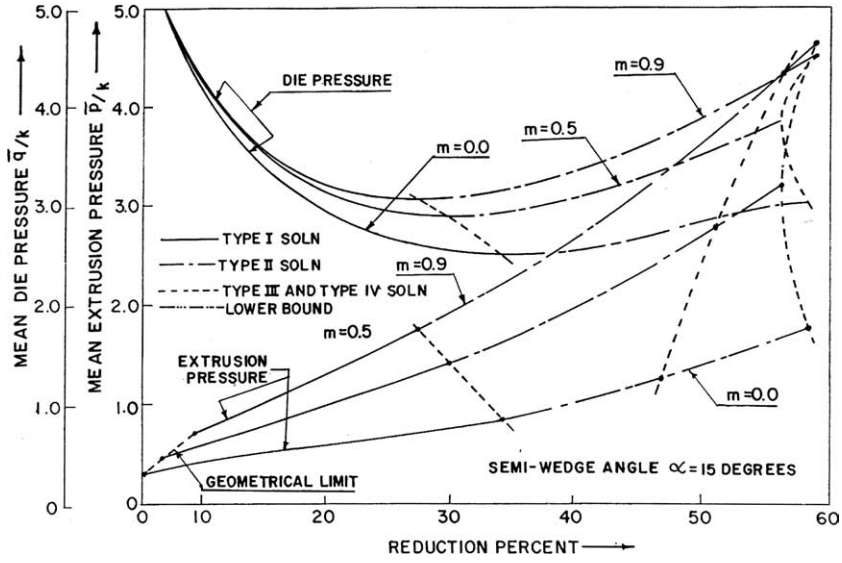

Fig. 5. Variation of mean extrusion and die pressures with percent reduction for different friction factors on die face semi-wedge angle = 15°.

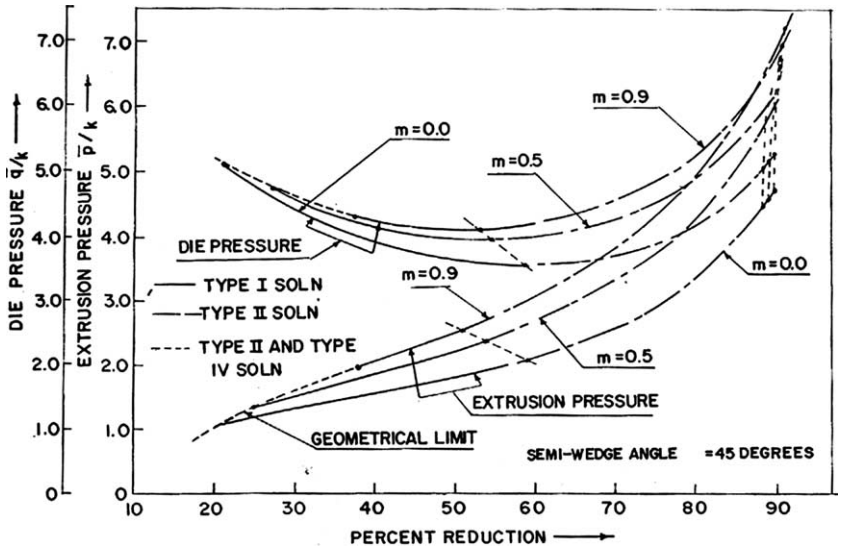

Fig. 6. Variation of mean extrusion and die pressures with percent reduction for different friction factors on die for semi-wedge angle = 45°.

5. Results and discussion

For any given value of λ, as θ (and ψ) increases, the reduction $(1 - h/H)$ increases from its limiting value corresponding to the limiting slipline field of Fig. 2(a) for type III solution, but decreases from its limiting value corresponding to the slipline field of Fig. 4(a) for type IV solution. For both solutions, ρ_1 decreases for fixed thickness, h, of the extruded sheet as θ increases and at a critical angle of $\theta(=\theta_E)$, ρ_1 eventually vanishes so that both solutions merge into the single eigen solution. The variation of θ_E with m is computed for different values of wedge angle α. Each θ_E is found to decrease from a maximum corresponding to the smooth dies ($m = 0$) to zero for perfectly rough dies ($m = 1$), where, the range of validity of these indirect solutions vanishes and the direct solution of Fig. 2 is valid for all reductions.

The variation of mean extrusion and die pressures with reduction is shown in Figs. 5,6 for die semi-angle α between 15° and 45° and for friction factor, m, between 0.3 and 0.9. In all cases, the reduction corresponding to the geometrical limit has been taken as the lower limit and the bulge limit, which slightly exceeds the geometrical limit for small wedge angles has been omitted for clarity. It may be seen from the above figures that the extrusion pressure increases due to friction at the billet-die interface and the effect is more evident at higher reductions. For any value of m, however, while the extrusion pressure increases monotonically with reduction, the die pressure first decreases from its limiting value corresponding to the geometrical limit, passes through a minimum corresponding to the limiting field of 1(a) and then increases through type II solution and in a quasi-oscillatory manner through type III and type IV solutions.

The effect of die angle α on mean extrusion pressure is shown in Figs. 7,8 for friction factor m between 0 and 0.9 and for fractional reductions between 30% and 60%. It may be seen from these figures that for any reduction

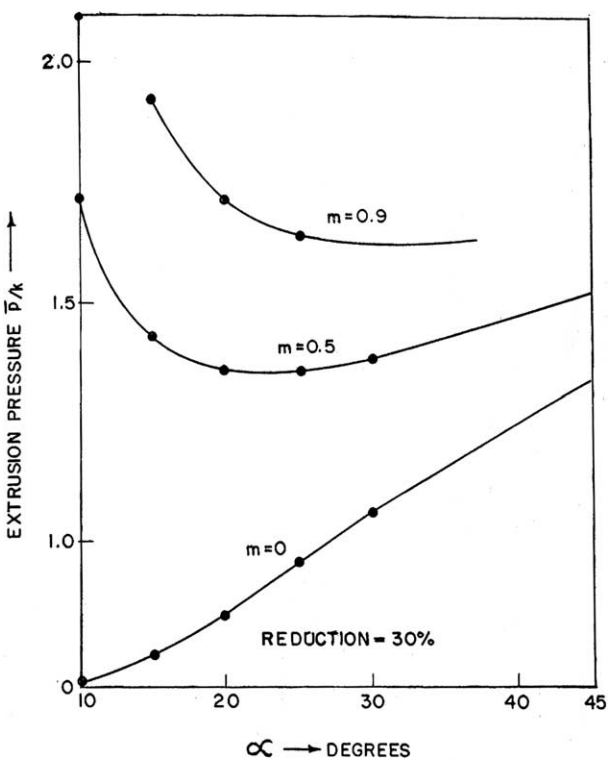

Fig. 7. Variation in value of optimum die angle with variation in friction factor for 30% reduction.

depending on the value of m, there is an optimum die angle for which the extrusion pressure is minimum and, its value for any reduction increases with in the value of m.

In Table 1 the results from the present analysis are compared with those of Chenot et. al. [10] for the case of axisymmetric extrusion with smooth dies. It is rather interesting to note that for reductions even upto 60% the maximum discrepancy in the two results does not exceed seven percent.

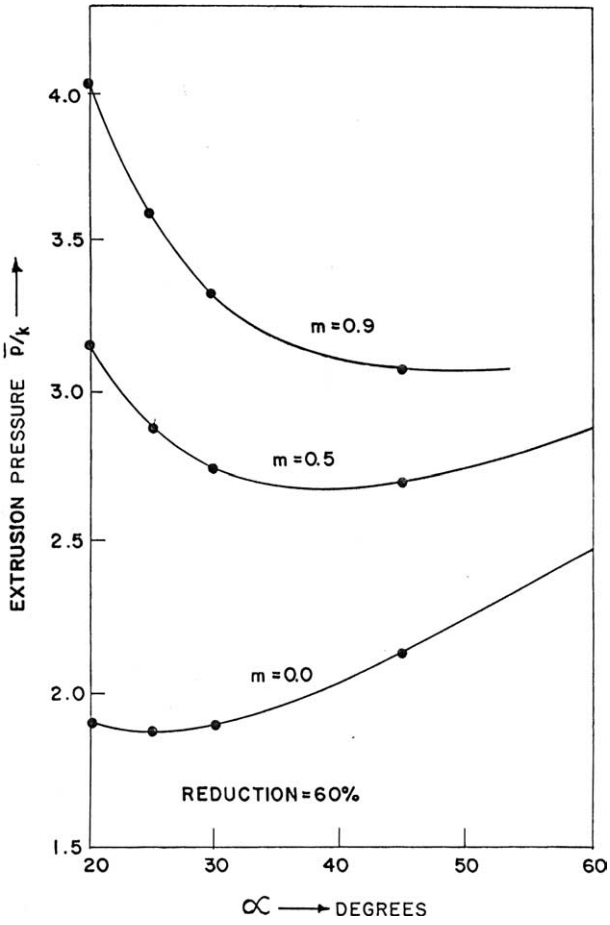

Fig. 8. Variation in value of optimum die angle with variation in friction factor for 60% reduction.

Table 1

Semi-wedge angle α in degree	Reduction percent	Mean extrusion pressure $\frac{\bar{p}}{y}$	
		Plane strain case (present analysis)	Axisymetric case [12]
10	20	0.28	0.3
20	40	0.62	0.63
30	40	0.73	0.76
45	40	0.91	0.94
30	60	1.1	1.1
45	60	1.23	1.3

6. Conclusion

1. The mean extrusion pressure increases with reduction. For type III and type IV solutions, the variation is quasi-oscillatory.
2. Extrusion pressure increases in the presence of friction and the effect is more evident at larger reductions.
3. For a given die angle, α, and friction factor, m, the die pressure is a minimum for the transition field between type I and type II solutions.
4. For smooth dies ($m = 0$), the maximum discrepancy between extrusion pressures for axisymmetric extrusion and that for sheet extrusion does not exceed 7% upto a reduction level of about 60%.
5. The value of the optimum die angle increases with increase in reduction and with increase in the value of the friction factor m.

References

[1] Nagpal V, Altan T. Analysis of three-dimensional metal flow in extrusion shapes With the use of dual stream functions. In: Proceedings of the third North American metal working research conference. Pittsburgh; 1975. p. 26–40.
[2] Narayanasamy R, Srinivasn P, Venkatesan R. Computer aided design and manufacture of streamlined extrusion dies. J Mater Proc Technol 2003;138:262–4.
[3] Kar PK, Sahoo SK, Das NS. Upper bound analysis for extrusion of T-section bar from square billet through square dies. Meccanica; 2001. p. 399–10.
[4] Maity KP, Kar PK, Das NS. A class of upper bound solutions for the extrusions of square shapes from square billets through curved dies. J Mater Proc Technol 1996;62:185–90.
[5] Narayanasamy R, Polonalagusamy R, Venkatesan R, Srinivasan P. An upper bound solution to extrusion of circular billet to circular shape through cosine dies. Mater Design; 2004 [in press].
[6] Hill R, Tupper SJ. A new theory of plastic deformation in wire drawing. J Iron Steel Inst 1948;159:353.
[7] Green AP. A theoretical investigation of the compression of a ductile material between smooth flat dies. Phil Mag 1951;42:900.
[8] Dewhurst P, Collins IF. A matrix technique for constructing slipline field solutions to a class of plane strain plasticity problems. Int J Num Meth Eng 1973;7:357.
[9] Venter RD, Hewitt RL, Johnson W. Application for the matrix inversion technique to extrusion and drawing problems. ASME Winter Meeting; 1978.
[10] Chenot JL, Felgeres L, Lavarenne B, Salencon J. A numerical application of the slipline field method to extrusion through conical dies. Int J Eng Sci 1978;16:263.
[11] Green AP, Hill R. Calculation on the influence of friction and die geometry in sheet drawing. J Mech Phys Solids 1952;1:31.
[12] Bishop JFW. Calculation on sheet drawing under back tensions through a rough wedge-shaped die. J Mech Phys Solids 1953;2:39.
[13] Johnson W. Extrusion through wedge-shaped dies. Part-I. J Mech Phys Solids 1955;3:218.
[14] Johnson W. Extrusion through wedge-shaped dies. Part-II. J Mech Phys Solids 1955;3:224.
[15] Green AP. Calculations on sheet drawing. BISRA Report No. MW/B/7/52; 1952.
[16] Westwood D, Wallace JF. Upper bound values of the loads on a rigid-plastic body in plane strain. J Mech Eng Sci 1960;2:179.